



HAL
open science

Next-Point Prediction for Direct Touch Using Finite-Time Derivative Estimation

Mathieu Nancel, Stanislav Aranovskiy, Rosane Ushirobira, Denis Efimov,
Sébastien Poulmane, Nicolas Roussel, Géry Casiez

► **To cite this version:**

Mathieu Nancel, Stanislav Aranovskiy, Rosane Ushirobira, Denis Efimov, Sébastien Poulmane, et al.. Next-Point Prediction for Direct Touch Using Finite-Time Derivative Estimation. Proceedings of the ACM Symposium on User Interface Software and Technology (UIST 2018), Oct 2018, Berlin, Germany. 10.1145/3242587.3242646 . hal-01893310

HAL Id: hal-01893310

<https://inria.hal.science/hal-01893310v1>

Submitted on 11 Oct 2018

HAL is a multi-disciplinary open access archive for the deposit and dissemination of scientific research documents, whether they are published or not. The documents may come from teaching and research institutions in France or abroad, or from public or private research centers.

L'archive ouverte pluridisciplinaire **HAL**, est destinée au dépôt et à la diffusion de documents scientifiques de niveau recherche, publiés ou non, émanant des établissements d'enseignement et de recherche français ou étrangers, des laboratoires publics ou privés.



Distributed under a Creative Commons Attribution 4.0 International License

Next-Point Prediction for Direct Touch Using Finite-Time Derivative Estimation

Mathieu Nancel^{1,2} Stanislav Aranovskiy³ Rosane Ushirobira^{1,2} Denis Efimov^{1,2}
Sébastien Poulmane^{1,2} Nicolas Roussel^{1,2} Géry Casiez^{2,1}

¹Inria, France ²Univ. Lille, UMR 9189 - CRISAL, Lille, France
³IETR, CentraleSupélec, Rennes, France

ABSTRACT

End-to-end latency in interactive systems is detrimental to performance and usability, and comes from a combination of hardware and software delays. While these delays are steadily addressed by hardware and software improvements, it is at a decelerating pace. In parallel, short-term input prediction has shown promising results in recent years, in both research and industry, as an addition to these efforts. We describe a new prediction algorithm for direct touch devices based on (i) a state-of-the-art finite-time derivative estimator, (ii) a smoothing mechanism based on input speed, and (iii) a post-filtering of the prediction in two steps. Using both a pre-existing dataset of touch input as benchmark, and subjective data from a new user study, we show that this new predictor outperforms the predictors currently available in the literature and industry, based on metrics that model user-defined negative side-effects caused by input prediction. In particular, we show that our predictor can predict up to 2 or 3 times further than existing techniques with minimal negative side-effects.

Author Keywords

touch input; latency; lag; prediction technique.

INTRODUCTION

End-to-end latency in interactive systems is the sum of all hardware and software delays (e.g. sensing, recognition, stored memory, rendering) between a physical input and the displaying of its effects (e.g. respectively a key press and the appearance of the corresponding letter on screen).

Current direct touch systems present end-to-end latencies ranging from 50 to 280 ms [3, 22]. These values are above perception thresholds and degrade performance. Previous studies have shown that users can notice end-to-end latencies as low as 2 ms with a pen [21] and 5 to 10 ms with a finger [22]. Performance is degraded from 25 ms in dragging tasks with a finger [12]. Deber et al. further show that improvements in latency as small as 8 ms are noticeable from a wide range of baseline latencies [12]. While we can expect

that next generations of touch interactive systems will exhibit less latency using, for example, higher frequency input and output, this comes at the cost of higher power consumption and its complete suppression seems unlikely.

In combination with latency reduction, latency *compensation* using next-point prediction techniques offers a promising avenue to cope with latency. In dragging tasks, these techniques use previous touch positions to predict the next ones in a near future in order to estimate the current finger position [20]. The existing prediction techniques are mainly based on Taylor series [5, 17, 25, 28, 29], Kalman filters [14, 16, 18, 26, 27], curve fitting [1], heuristic approaches [13], and neural networks [10, 11]. Only a few of them have been evaluated [5, 10]. Nancel et al. have shown that input prediction introduces noticeable side-effects such as jitter or spring-effect. They characterized and proposed metrics to measure these side-effects [20]. They report that participants perceived latency as less disturbing than the side-effects introduced by current prediction techniques when trying to fully compensate latency. As a result, next-point prediction techniques can only be useful if they can compensate some of the latency while minimizing the side-effects they introduce.

We contribute a new prediction algorithm for direct touch devices designed to offer good trade-offs between latency reduction and side-effects. It is based on a state-of-the-art, finite-time differentiator that provides estimation of the first, second and third time derivatives of the input position in a predefined, limited time. It is combined with a smoothing mechanism that dampens the amplitude of the prediction depending on the user's input speed, to minimize jitter [4, 20].

Using a pre-existing large dataset of touch input as benchmark, we show that this new predictor outperforms the predictors currently available in the literature and industry for direct touch input, based on metrics that model user-defined negative side-effects caused by input prediction. These results were then confirmed in a controlled user experiment.

The paper makes the following contributions:

- the introduction of the HOM finite-time derivative estimator to the HCI community, to go beyond computing derivatives limited to straightforward calculations,
- the adaptation of HOM to include a speed-based smoothing mechanism, and its first application to latency compensation with direct touch,
- the design and application of an optimization algorithm for the parameters of a HOM-based input predictor that can be adapted to system and user requirements,
- the validation of a stroke dataset from the literature to serve as benchmark for new predictors (in appendix),
- the formulation of a unique metric for the benchmarking of input prediction algorithms,
- an extensive, simulation-based validation of the resulting technique against state-of-the-art input predictors,
- a user experiment providing subjective comparison of our prediction technique against state of the art predictors, for different tasks and levels of compensation.

After addressing the related work we describe our prediction technique before detailing its evaluation.

RELATED WORK

Our review of the related work first covers measures and human factors related to end-to-end latency on direct touch surfaces before detailing current next-point prediction techniques and time derivative estimation methods.

End-to-end Latency in Direct Touch

In 2012 Ng et al. measured latency on various touch devices and found end-to-end latencies ranging from 60 to 200 ms [22]. More recently Casiez et al. found end-to-end latency on current touch devices ranging from 48 to 276 ms and show it is affected by the hardware, operating system and toolkit [3]. The authors further show that the input latency (time from a physical action of the user on an input device to the reception of the corresponding event by the system) is in the range 14 to 25 ms using native toolkits on Android devices and that most of the end-to-end latency comes from the output latency (time elapsed between calling the repaint of the display and its actual update) which is affected by the operating system, graphic card and physical screen.

The impact of end-to-end latency on user perception and performance in direct touch interaction is well covered in the literature. For dragging tasks, users can reliably perceive touch-screen latency as low as 5-10 ms [22] as they can easily notice the physical distance between their finger and the associated visual stimulus [6]. For tapping tasks, the perception threshold is higher at 24 ms [12]. The thresholds are even lower using a pen. Ng et al. reported 2 ms for dragging and 6 ms for scribbling [21]. Jota et al. showed that performance is affected from 25 ms in dragging tasks with a finger [12].

To sum up, current systems show latencies above perception and performance thresholds. Ideally even the most efficient systems showing 50 ms latency should reduce their latency

by 25 ms to prevent human performance degradation, and by 40 ms to make the latency un-noticeable. Deber et al. have also shown that improvements in latency as small as 8 ms are noticeable from a wide range of baseline latencies [12]. If one can expect current hardware will improve in a near future to reduce latency, its complete suppression is unlikely.

Next-point Prediction Techniques

Nancel et al. [20] detailed existing related work on next-point prediction techniques that fall into four main categories: Taylor series [5, 17, 25, 28, 29], Kalman filter [14, 16, 18, 26, 27], curve fitting [1] and heuristic approaches [13]. See Nancel et al. for a detailed description of these techniques [20]. More recently Henze et al. used neural networks for prediction and found their technique to be more precise than first-, second- and third-order polynomial extrapolations [10, 11]. Their neural networks were trained on a very large data collection. We could unfortunately not integrate this technique in our study, as the data and code to train new networks to our experiment's latencies and device were not available at the time. The approach in [11] and the one presented in this article thus remain to be compared.

If current next-point prediction techniques can compensate some of the latency, they also introduce prediction artifacts. Nancel et al. characterized the side-effects introduced by these techniques and noticed by participants and classified them in 7 categories: lateness, over-anticipate, wrong distance, wrong orientation, jitter, jumps, and spring effect [20]. In addition they developed quantitative metrics that correlate positively with the frequency of perceived side-effects.

With the exception of the curve fitting and neural networks techniques, all other techniques rely on the use of speed and acceleration determined from the finger positions. These derivatives are estimated using simple time differentiation based on the two previously acquired positions or computed speeds. Simple time differentiation techniques have the benefit of being straightforward to implement and fast to execute. Furthermore they use the most recent information available and thus introduce a small latency in the estimation of speed or acceleration. However the resulting computation of speed and acceleration are generally noisy, which results in higher chances to notice side-effects. Yet, more advanced techniques to estimate derivatives also exist.

Time Derivative Estimation Techniques

Numerical differentiation is a key issue in the domains of signal processing and control engineering as it appears in many problems where a noisy signal needs to be reconstructed or filtered. There are many methods providing numerical differentiation with different levels of performance (the most important of them being sensitivity to measurement noises, computational complexity, and estimation delay). Popular techniques include statistical approaches such as the minimum least squares method [7]. In recent years, novel deterministic approaches have been proposed yielding good results in terms of robustness to noise and computational aspects. In this framework, we may cite the approach based on the sliding mode methods [8, 15], algebraic methods [9, 24] or

the homogeneous systems method [19, 23]. Minimum least squares and sliding mode approaches either have to be computed off-line, or present significant chattering, defined as an *undesirable phenomenon of oscillations with finite frequency and amplitude*. Algebraic methods are robust to noise but introduce some delay in the estimations. The homogeneous-based differentiator has a fast rate of convergence and good robustness with respect to disturbances. It appears as the most appropriate numerical differentiation technique in the context of latency compensation. In the following we refer to this technique as ‘HOM’, short for *homogeneous*.

We clarify that the HOM finite-time derivative estimator is not a next-point prediction algorithm. It is a general-purpose method introduced in 2008 [23], initially to secure communications. This paper is highly cited in the control theory community, showing the method’s applicability in various contexts, but never for latency compensation until 2016 [24].

In [24], the HOM differentiator was compared to other differentiators for basic latency compensation with a mouse. However that involved minimal validation, using small datasets and simplistic metrics based on predicted-to-actual distances; such metrics were later shown to be limited and possibly misleading [20]. Therefore the results in [24] remain to be confirmed, especially for direct touch for which latency can be more noticeable than with a mouse. HOM has never been used for latency compensation with direct touch. In fact, despite its 10 years of existence it was never brought to the HCI literature, in which the typical method to compute derivatives remains mostly limited to straightforward calculations of the form $(p_i - p_{i-1})/(t_i - t_{i-1})$ relative to the last input event i , where p_i is the value of the signal at the instant t_i .

Another approach based on finite impulse response (FIR) filters has been proposed recently in [2]. It demonstrates good robustness properties with respect to measurement noise, but still requires more computational capacities (involves matrix manipulations with 16 times 16 matrices for both X and Y) without a corresponding quality of differentiation improvement comparing to HOM differentiator. In addition the FIR has at least 16 tunable gains for each axis, against 5 for HOM.

THE TURBOTOUCH PREDICTOR

Given a measured position¹ $x_m(t_k)$ at a time t_k , the TURBOTOUCH predictor (TTP) algorithm² attempts to estimate a real object’s position $x(t_k)$ using features of the ongoing trajectory. The measured position is always sensed with a certain latency L :

$$x_m(t_k) = x(t_k - L)$$

In practice the value L is not constant, but for algorithm design and performance evaluation purposes we impose the assumption that an averaged constant value L_0 is available. Therefore, we can define the estimation error $e(t_k)$ between the real position $x(t_k)$ and its estimate $\hat{x}(t_k)$:

$$e(t_k) = x(t_k) - \hat{x}(t_k) \approx x_m(t_k + L_0) - \hat{x}(t_k)$$

¹The calculations that follow are described for the x coordinate only for simplicity, and must be performed for y as well in real use.

²Our prediction algorithm and tuning process are available at ns.inria.fr/loki/TTP/.

The approximate equality becomes exact assuming $L_0 = L$, in such a case the error between the real position $x(t_k)$ and the estimate $\hat{x}(t_k)$ is exactly the difference between the further measured position $x_m(t_k + L_0)$ and the estimate $\hat{x}(t_k)$.

Perhaps intuitively, there exists a trade-off between high-frequency oscillations of the predicted cursor, or “jitter”, and how promptly a predicted cursor reacts to quick changes in trajectory or in speed. This trade-off is more noticeable when large amounts of latency need to be compensated. Nancel et al. [20] reported that:

- estimators that use only the most recent measured positions tend to react faster to input change, but increase the chances of cursor jitter. Using points further away in the past lowers the risk of jitter, but delays the cursor’s response to sudden changes of input speed and direction,
- participants’ reports of jitter were negatively correlated with reports of “lateness” of the cursor, from which we infer that compensating smaller amounts of latency lowers the risks of noticeable jitter, but increase the noticeable lag,
- participants reported more jittery cursor movements when moving slowly. No correlation was observed between slow movements and reported “lateness”, but it is trivial to calculate that, for a constant latency, lower speeds result in smaller—and therefore less noticeable—offsets.

To summarize, when most of the latency is to be compensated, estimations calculated from most “recent” measures react faster to sudden changes of trajectory, but increase the chances of jitter. Jitter, however, is more noticeable when the user is moving slowly.

To cope with the aforementioned trade-off, the main feature of the proposed design is that the prediction is smoothly turned off when the instant velocity of the controlled object, further denoted as $V(t)$, is sufficiently low. This simultaneously limits jitter with admissibly small prediction error for low velocities, and provides fast cursor reactions for medium and high velocities.

The proposed estimator behaves according to the following rules, where V_{low} is a general parameter.

- If $V(t_k) \geq V_{low}$, then the predictor behaves normally by extrapolating from the most recent features of the trajectory.
- If $V(t_k) < V_{low}$, then the main goal of the estimator is to avoid any noise amplification, and a good strategy is to turn off estimation and bypass the measurements.
- To avoid discontinuities (*jumps*) in estimation, the switching is smoothed with an exponential weighting function.
- Finally, to remove any remaining noise in the predicted positions, we apply a light filtering using the 1ϵ filter [4].

Estimator Description

We use the estimator

$$\hat{x}(t_k) = x_m(t_k) + \alpha(t_k) \left(\hat{\phi}_x^\top(t_k) \cdot \theta_x \right) \quad (1)$$

where $(\hat{\phi}_x^\top(t_k) \cdot \theta_x)$ is the estimation of the input movement since the most recently measured position $x_m(t_k)$. It is composed of an estimate of the vector of time derivatives

$$\hat{\phi}_x(t_k) := [x_m^{(1)}(t_k), x_m^{(2)}(t_k), x_m^{(3)}(t_k)]^\top$$

and a constant gain vector $\theta_x \in \mathbb{R}^4$ obtained by off-line optimization (see below). $\alpha(t_k) \in \mathbb{R}^+$ is the exponential weighting function that implements the smoothing mentioned above.

The estimate $\hat{\phi}_x(t_k)$ is computed using HOM [23].

$$\begin{aligned} s_x(t_k) &= \text{HOM}(s_x(t_{k-1}), x_m(t_k), \alpha_x, \lambda_x, \Delta_t), \\ \hat{\phi}_x(t_k) &= [s_{x,2}(t_k), s_{x,3}(t_k), s_{x,4}(t_k)]^\top, \end{aligned} \quad (2)$$

where $s_x(t_k)$ is the state vector of the differentiator, $\alpha_x > 0$ and $\lambda_x \in [-0.2, 0]$ are the differentiator's parameters obtained by off-line optimization (see below), and Δ_t is the integration interval, a general parameter. The HOM is a discrete-time approximation of the continuous-time differential equation

$$\begin{bmatrix} \dot{s}_{x,1}(t_k) \\ \dot{s}_{x,2}(t_k) \\ \dot{s}_{x,3}(t_k) \\ \dot{s}_{x,4}(t_k) \\ \dot{s}_{x,5}(t_k) \end{bmatrix} = \begin{bmatrix} s_{x,2}(t_k) - 5\alpha_x |\varepsilon_x(t_k)|^{1+\lambda_x} \text{sign}(\varepsilon_x(t_k)) \\ s_{x,3}(t_k) - 10\alpha_x^2 |\varepsilon_x(t_k)|^{1+2\lambda_x} \text{sign}(\varepsilon_x(t_k)) \\ s_{x,4}(t_k) - 10\alpha_x^3 |\varepsilon_x(t_k)|^{1+3\lambda_x} \text{sign}(\varepsilon_x(t_k)) \\ s_{x,5}(t_k) - 5\alpha_x^4 |\varepsilon_x(t_k)|^{1+4\lambda_x} \text{sign}(\varepsilon_x(t_k)) \\ -\alpha_x^5 |\varepsilon_x(t_k)|^{1+5\lambda_x} \text{sign}(\varepsilon_x(t_k)) \end{bmatrix} \quad (3)$$

with $s_{x,i}$ the i -th element of s_x , and $\varepsilon_x(t_k) = s_{x,1}(t_k) - x_m(t_k)$.

The exponential weighting function $\alpha(t_k)$ above is computed as

$$\alpha(t_k) = \alpha(t_{k-1}) + \gamma_\alpha (\alpha^*(t_k) - \alpha(t_{k-1})) \quad (4)$$

with $0 < \gamma_\alpha < 1$ a general parameter and

$$\alpha^*(t_k) = \begin{cases} 1 & \text{if } V(t_k) \geq V_{low}, \\ 0 & \text{if } V(t_k) < V_{low}. \end{cases} \quad (5)$$

The estimator's constant gain vector θ_x is obtained via off-line minimization of the estimation cost function defined below.

Readers will have noted that neither the actual latency L nor the expected average latency L_0 appear in the computations above. This is because L_0 is a parameter of the training process in which the values of α_x , λ_x , and θ_x are optimized (see below). These values therefore correspond to a specific input-output setup (from which the training data is gathered) as well as a specific amount of latency compensation. Compensating for a new latency therefore requires to run a new optimization.

Note also that the parameters α_x , λ_x and θ_x are obtained through an optimization process whose main purpose is to minimize metrics of prediction error, not to estimate speed, acceleration, and jerk as closely as possible to physical units. For that reason, the estimates $\dot{s}_{x,n}(t_k)$ need to be remapped to physical scales before they can be used as estimations of speed, acceleration, or jerk, e.g. in Eq. 5: $V_x(t_k) = \mu \times s_{x,2}(t_k)$. The parameter μ is obtained through off-line optimization (see below).

Switched Estimator Algorithm

We now describe every step of a typical, real-time use of our switched estimator algorithm. For the sake of simplicity and understanding the algorithm is described in a 2D context but

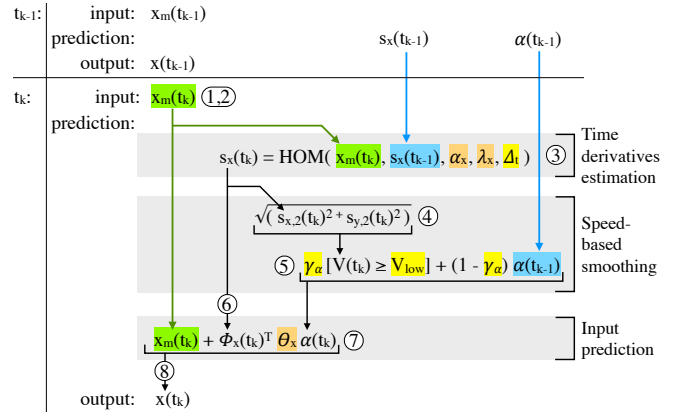


Figure 1: General description of real-time prediction process, with step numbers. Input in green, previously computed variables in blue, general parameters in yellow, optimized parameters in orange.

could be easily extended in 3D. It can also be adapted for rotations or any other input channel used for pointing.

Input signals. At each step the input signals are the time instance t_k and the measurements $x_m(t_k)$, $y_m(t_k)$.

Output signals. At each step the output signals are the estimations $\hat{x}(t_k)$, $\hat{y}(t_k)$.

Parameters. The estimator has the following parameters:

- the HOM parameters:

$$\begin{aligned} \alpha_x, \alpha_y &> 0, \\ \lambda_x, \lambda_y &\in [-0.2, 0], \\ \Delta_t &> 0 \text{ (integration time step)} \end{aligned}$$

- the gains $\theta_x, \theta_y \in \mathbb{R}^3$,
- the HOM conversion ratio μ ,
- the velocity threshold $V_{low} \geq 0$,
- the smoothing parameter $0 < \gamma_\alpha < 1$.

Internal variables. The internal variables of the estimator are the timer variable $\tau \in \mathbb{R}$, the differentiator states $s_x, s_y \in \mathbb{R}^5$, and the weighting variable $\alpha \in \mathbb{R}$.

Initialization. At the first time instance t_1 set

$$\begin{aligned} \tau &= t_1, \\ s_x(t_1) &= [x_m(t_1), 0, 0, 0, 0]^\top, \\ s_y(t_1) &= [y_m(t_1), 0, 0, 0, 0]^\top, \\ \alpha(t_1) &= 0, \\ \hat{x}(t_1) &= x_m(t_1), \\ \hat{y}(t_1) &= y_m(t_1). \end{aligned}$$

Estimation. At each time instance t_k , $k > 1$:

Step 1. Get the new measurements.

Step 2. Pre-process the measurements. This step includes: input data verification, units conversion and time frames adjustment between the estimator and the

measurements provider. The output of this step are the preprocessed values t_k , $x_m(t_k)$ and $y_m(t_k)$.

Step 3. Update the internal variable τ and the states $s_x(t_k)$, $s_y(t_k)$ as follows:

- (a) Set $s_x(t_k) = s_x(t_{k-1})$ and $s_y(t_k) = s_y(t_{k-1})$.
- (b) While $\tau < t_k$, repeat:
 - i. Compute $\varepsilon_x(t_k) = s_{x,1}(t_k) - x_m(t_k)$ and $\varepsilon_y(t_k) = s_{y,1}(t_k) - y_m(t_k)$, where $s_{x,i}$ and $s_{y,i}$ are the i -th elements of the vectors s_x and s_y , respectively.
 - ii. Update

$$s_x(t_k) = s_x(t_k) + \begin{bmatrix} s_{x,2}(t_k) - 5\alpha_x |\varepsilon_x(t_k)|^{1+\lambda_x} \text{sign}(\varepsilon_x(t_k)) \\ s_{x,3}(t_k) - 10\alpha_x^2 |\varepsilon_x(t_k)|^{1+2\lambda_x} \text{sign}(\varepsilon_x(t_k)) \\ s_{x,4}(t_k) - 10\alpha_x^3 |\varepsilon_x(t_k)|^{1+3\lambda_x} \text{sign}(\varepsilon_x(t_k)) \\ s_{x,5}(t_k) - 5\alpha_x^4 |\varepsilon_x(t_k)|^{1+4\lambda_x} \text{sign}(\varepsilon_x(t_k)) \\ -\alpha_x^5 |\varepsilon_x(t_k)|^{1+5\lambda_x} \text{sign}(\varepsilon_x(t_k)) \end{bmatrix} \Delta_t$$

and

$$s_y(t_k) = s_y(t_k) + \begin{bmatrix} s_{y,2}(t_k) - 5\alpha_y |\varepsilon_y(t_k)|^{1+\lambda_y} \text{sign}(\varepsilon_y(t_k)) \\ s_{y,3}(t_k) - 10\alpha_y^2 |\varepsilon_y(t_k)|^{1+2\lambda_y} \text{sign}(\varepsilon_y(t_k)) \\ s_{y,4}(t_k) - 10\alpha_y^3 |\varepsilon_y(t_k)|^{1+3\lambda_y} \text{sign}(\varepsilon_y(t_k)) \\ s_{y,5}(t_k) - 5\alpha_y^4 |\varepsilon_y(t_k)|^{1+4\lambda_y} \text{sign}(\varepsilon_y(t_k)) \\ -\alpha_y^5 |\varepsilon_y(t_k)|^{1+5\lambda_y} \text{sign}(\varepsilon_y(t_k)) \end{bmatrix} \Delta_t$$

- iii. Update $\tau = \tau + \Delta_t$.

Step 4. Compute the estimate of 2D velocity absolute value

$$\hat{V}(t_k) = \mu \sqrt{(s_{x,2}(t_k))^2 + (s_{y,2}(t_k))^2},$$

and α^* as

$$\alpha^*(t_k) = \begin{cases} 1 & \text{if } V(t_k) > V_{low}, \\ 0 & \text{if } V(t_k) \leq V_{low}. \end{cases}$$

Step 5. Update the internal variable α as

$$\alpha(t_k) = \alpha(t_{k-1}) + \gamma_\alpha (\alpha^*(t_k) - \alpha(t_{k-1})).$$

Step 6. Define the estimates of derivatives

$$\hat{\phi}_x(t_k) = [s_{x,2}(t_k), s_{x,3}(t_k), s_{x,4}(t_k)]^\top,$$

$$\hat{\phi}_y(t_k) = [s_{y,2}(t_k), s_{y,3}(t_k), s_{y,4}(t_k)]^\top.$$

Step 7. Compute the estimates

$$\hat{x}(t_k) = x_m(t_k) + \alpha(t_k) \hat{\phi}_x^\top(t_k) \theta_x,$$

$$\hat{y}(t_k) = y_m(t_k) + \alpha(t_k) \hat{\phi}_y^\top(t_k) \theta_y.$$

Step 8. Post-process the estimates. This step includes units conversion and time frames adjustment between the estimator and an output device.

Implemented in C++, the above algorithm results in about 150 lines of code without the use of any external function. One prediction takes 1.5 μ s on average (95th percentile = 2 μ s, max = 44 μ s) on an i7 4GHz processor, a few orders of magnitude below the amount of latency considered.

Parameters Tuning

The parameters used in the algorithm can be divided into two groups: the general parameters and the optimization-based parameters. The general parameters are tuned manually, taking into account physical and hardware specifications of the exact estimation problem and input/output devices. The optimization-based parameters are tuned using a given dataset of movements specific to the considered estimation problem, minimizing metrics described below.

General Parameters

The general parameters used at runtime are the integration interval $\Delta_t > 0$ and the parameters of the speed-based smoothing: the velocity threshold $V_{low} \geq 0$ and the smoothing gain $\gamma_\alpha \in]0, 1[$. V_{low} depends on visual tolerance, γ_α on behavior change tolerance, and Δ_t on computational capabilities, as detailed below.

- Δ_t is less or equal to the measurement period T_s . This value is a trade-off between computational time and accuracy, and depends on the target hardware. It is typically expressed as a proportion p of the system's average sampling period: $\Delta_t = p \cdot T_s$. For example, in our benchmark below we use the whole period ($p = 1$) on a sampling frequency of 120 Hz, so $\Delta_t = 1 \times 1000/120 = 8.33$ ms.
- V_{low} defines the minimum velocity at which the estimator is activated. It corresponds to the input speed below which the system latency is considered not noticeable; in our case, when the visual lag is hidden under the finger. The general idea is to switch the estimator on at a velocity for which the lag becomes noticeable to most users. The following formula is proposed for its adjustment:

$$V_{low} = \frac{E_{max}}{L_0},$$

where E_{max} is the maximal admissible error in distance units. For example, if we assume that the end-to-end latency is 68 ms and a typical user is affected by a deviation greater than 7 mm (as an estimation of finger radius), then a reasonable choice would be $V_{low} = \frac{7\text{mm}}{68\text{ms}} \approx 100$ mm/s. The value of V_{low} may be updated given users feedback.

- $0 < \gamma_\alpha < 1$ defines the exponential smoothing transient decay time,

$$\gamma_\alpha = 1 - 0.05 \frac{T_s}{t_{transients}},$$

where $t_{transients}$ is the admissible transient time of switching between two modes of the estimator. Assuming a desired transient time of 0.33 ms with 120 Hz sampling frequency, the corresponding value of γ_α is computed as

$$\gamma_\alpha = 1 - 0.05 \frac{8.33\text{ms}}{0.33\text{s}} \approx 0.73.$$

These rule-of-thumb formulae define initial values for our general parameters and we found them to work well in practice. These parameters could benefit from empirical tuning or extended exploration of their range and effects, but this is left to future work.

Two other general parameters are used in the optimization of the other predictor's parameters (see below):

- The expected average lag value L_0 . The shifted measurements $x_m(t_k + L_0)$ are further used to optimize the estimator's parameters.
- The jitter lower frequency bound F_b is the oscillation frequency above which cursor movements are interpreted as undesirable jitter. Along with F_b we consider HFG_{low} and HFG_{high} , the jitter amplification levels considered as "low" and "high", see below for the details on amplification level computation procedure. Based on our experiments these values are chosen as $F_b = 7\text{Hz}$, $HFG_{low} = 5$ and $HFG_{high} = 6$.

Optimized Parameters

The parameters tuned via optimization are the time differential gains $\theta_x, \theta_y \in \mathbb{R}^3$, the HOM conversion ratio μ , and the HOM differentiator parameters $\alpha_x, \alpha_y \in \mathbb{R}^+$ and $\lambda_x, \lambda_y \in [-0.2, 0]$. Note that HOM has been used in very different domains, and many application-related methods have been developed to tune its parameters. Our tuning protocol follows the general principles of these existing methods, but is adapted to the specific problem of latency compensation.

The estimation algorithm considers each axis separately, so the corresponding parameters are optimized separately as well. However, the tuning procedure is the same. Below we describe the tuning procedure for the x axis only.

The input data set \mathcal{D} consists of equally spread time instances t_k and the corresponding measurements $x_m(t_k)$, $k = 1, \dots, N$. For the tuning procedure it is assumed that a sufficiently large data set is available representing all kinds of possible / admissible movements.

Metrics used

- The high-frequency gain $HFG(\hat{x})$ represents how the estimator amplifies the input oscillation frequencies above F_b with respect to the measured position. We compute this value as follows. First, using fast Fourier transform (e.g. Matlab's `fft` function) we remove from the signals \hat{x} and x_m all the components below the frequency F_b . Then, the ratio of the \mathcal{L}_1 norms of the filtered signals is computed and considered as the noise amplification level.
- The mean average estimation error is computed as

$$E_1(\hat{x}) = \frac{1}{N - N_0} \sum_{i=1}^{N-N_0} |x_m(t_i + L_0) - \hat{x}(t_i)|,$$

where N_0 is the maximum integer below $\frac{L_0}{T_s}$, i.e. latency value expressed in number of sampling intervals. The mean average error with respect to no estimation, is further denoted as

$$E_1^0 = \frac{1}{N - N_0} \sum_{i=1}^{N-N_0} |x_m(t_i + L_0) - x_m(t_i)|.$$

- The maximum estimation error is computed as

$$E_\infty(\hat{x}) = \max_i |x_m(t_i + L_0) - \hat{x}(t_i)|.$$

The maximum error with respect to no estimation, is further denoted as

$$E_\infty^0 = \max_i |x_m(t_i + L_0) - x_m(t_i)|.$$

- The cost function $J(\hat{x})$ of the estimation is computed as

$$J(\hat{x}) = \kappa_1 J_1(\hat{x}) + \kappa_2 J_2(\hat{x}) + \kappa_3 J_3(\hat{x}),$$

where $\kappa_1 > 0$, $\kappa_2 > 0$ and $\kappa_3 > 0$ are tuning constants and

$$J_1(\hat{x}) = \frac{E_1(\hat{x})}{E_1^0},$$

$$J_2(\hat{x}) = \frac{E_\infty(\hat{x})}{E_\infty^0},$$

$$J_3(\hat{x}) = \begin{cases} 0 & \text{if } HFG_{high} \leq HFG(\hat{x}) \\ \frac{HFG(\hat{x}) - HFG_{low}}{HFG_{high} - HFG_{low}} & \text{if } HFG_{low} < HFG(\hat{x}) < HFG_{high} \\ 1 & \text{if } HFG(\hat{x}) \leq HFG_{low} \end{cases}$$

In our experiments we have $\kappa_1 = \kappa_2 = \kappa_3 = 1$. However, these values can be modified given user experience feedback.

Parameter tuning

With the above, for any given estimate \hat{x} we can compute the performance index $J(\hat{x})$. Our goal is to find values for the parameters α_x , λ_x , and θ_x that produce predictions that minimize this performance index over the given dataset \mathcal{D} . Recall that the parameters α_x and λ_x are used to compute the output $\hat{\phi}_x$ of the HOM differentiator (2), so we can write

$$\hat{\phi}_x(t_k) = \hat{\phi}_x(t_k | \alpha_x, \lambda_x),$$

and θ_x is used to compute the estimate \hat{x} , see (1),

$$\hat{x}(t_k | \alpha_x, \lambda_x, \theta_x) = x_m(t_k) + \alpha(t_k) \hat{\phi}_x^\top(t_k | \alpha_x, \lambda_x) \theta_x.$$

We therefore use two optimization loops. The inner loop considers α_x and λ_x as input parameters and attempts to find the best θ_x for the given dataset \mathcal{D} and HOM output $\hat{\phi}_x(t_k | \alpha_x, \lambda_x)$. The output of this inner loop is defined as $J_{inner}(\alpha_x, \lambda_x)$, the lowest cost function score for the chosen α_x and λ_x . The second, outer loop searches for α_x and λ_x using the best output of the inner loop.

The tuning algorithm is described as follows.

1. Define the dataset \mathcal{D} and choose initial guesses for α_x, λ_x .
2. For the chosen α_x, λ_x compute $\hat{\phi}_x(t_k | \alpha_x, \lambda_x)$ for all t_k .
3. Perform the inner loop optimization for the chosen α_x, λ_x and compute $J_{inner}(\alpha_x, \lambda_x)$.
 - 3.A. Choose initial guess for θ_x .
 - 3.B. Compute the estimate $\hat{x}(t_k | \alpha_x, \lambda_x, \theta_x)$ for all t_k .
 - 3.C. Compute the estimate cost function $J(\hat{x} | \alpha_x, \lambda_x, \theta_x)$.
 - 3.D. Update θ_x in order to decrease the cost function value.

3.E. Repeat steps 3B-3D until the optimal (minimum) value of $J(\hat{x}|\alpha_x, \lambda_x, \theta_x)$ is obtained. Define the corresponding value of θ_x as θ_x^{opt} .

3.F. Compute³ $J_{inner}(\alpha_x, \lambda_x) = J(\hat{x}|\alpha_x, \lambda_x, \theta_x^{opt})$.

4. Update α_x, λ_x in order to decrease the value of $J_{inner}(\alpha_x, \lambda_x)$.

5. Repeat steps 2-4 until the optimal (minimum) value of $J_{inner}(\alpha_x, \lambda_x)$ is obtained⁴. Define the corresponding values of α_x as α_x^{opt} and of λ_x as λ_x^{opt} .

6. Calculate μ as the inverse slope of the linear regression with null intercept between the instantaneous input speed $V(t_k) = \frac{\sqrt{(x_k - x_{k-1})^2 + (y_k - y_{k-1})^2}}{t_k - t_{k-1}}$ and HOM's first derivative estimation $\hat{V}(t_k) = \sqrt{(s_{x,2}(t_k))^2 + (s_{y,2}(t_k))^2}$ from the last iteration of step 3E, using the whole training dataset.

The obtained values $\alpha_x^{opt}, \lambda_x^{opt}$ and the corresponding optimized gains θ_x^{opt} are the desired estimator's parameters.

Finally, the predicted positions are smoothed using the 1€ filter in two steps. First, we filter the distance between the last detected input location (x_m, y_m) and the HOM estimate (\hat{x}, \hat{y}) , and adjust the predicted point according to that smoothed distance without changing its orientation from (x_m, y_m) . The idea is to limit back-and-forth oscillations of the prediction, e.g. due to extrapolation of measurement errors, without introducing a delay in responding to changes of direction. Second, we filter the coordinates of the resulting position to reduce the remaining jitter. For simplicity, the same parameters are used for the 1€ filter in both steps. The parameters we use correspond to very light filtering, to avoid introducing latency, but in practice they result in a noticeable reduction of jitter without sacrificing reactivity to direction change.

BENCHMARK VALIDATION

To validate our approach, we compared our predictor against existing predictors in the literature and industry, and for different levels of latency compensation. Previous work [20] showed that simple distance-based metrics only cover a small part of the negative side-effects caused by input prediction, and can even correlate negatively with some of them. Asking participants to systematically describe what is wrong with each predictor, in each task, and for each level of latency, is a tedious process: trying and commenting on each condition takes a lot of time. Such a study protocol would either have limited repetitions, or increased chances of fatigue effects.

Instead, we used the dataset of touch input events described in [20] and made available online⁵ so other practitioners can quickly simulate and evaluate new input predictors. This dataset consists of 6,454 input strokes (touch-down to touch-up) from 12 different participants, about one hour each, performing three tasks: panning, target docking, and drawing.

³The steps 3B-3E can be realized with a proper unconstrained optimization toolbox, e.g. `fminsearch` in Matlab.

⁴The steps 2-5 can be realized with a proper constrained optimization toolbox, e.g. `fmincon` in Matlab.

⁵<http://ns.inria.fr/mjolnir/predictionmetrics/>

See Appendix for an analysis of the input data's independence to the predictors that were active at the time of capture.

To compare these predictors, we also used 6 side-effect-modelling metrics from the same article:

Metric	$Mo(D)$	Description
Lateness	1	“late, or slow to react”
Over-anticipation	4	overreaction, “too far ahead in time”
Wrong orientation	4	compared to input motion
Jitter	5	“trembling around the finger location”
Jumps	5	“jumping away from the finger at times”
Spring Effect	2	“yo-yo around the finger”

Table 1: Negative side-effects reported by participants in [20]. $Mo(D)$ are the modes of how Nancel et al.'s participants rated each side-effect in terms of disturbance, between 1 (“Not disturbing at all”) and 5 (“Unbearable / Unacceptable”), taken from Table 1 in [20].

These metrics take sets of input- and predicted coordinates as input, and return scalar values of arbitrary scales, that have been shown to correlate linearly with the probability that participants report the corresponding side-effect. We reused the linear functions reported in Table 5 in [20] to obtain these probabilities.

In all of what follows, and similar to the authors' treatment in [20], we discarded the 5% shortest and 5% longest strokes of the dataset in duration.

Simulation-based Comparison

We compared our own predictor (TTP), the Double-Exponential Smoothing Predictor (DESP) from LaViola [14], and 4 out of the 5 predictors presented in [20] (not counting the control condition without prediction) (Table 2). The remaining predictor is KALMAN which in [20] behaved comparably to the control condition (no prediction). The authors hypothesized that “Assuming most predictions were observed to have a low accuracy [...] the predictor would rely very little on its own predictions” (p. 277).

Name	Working principle	From
FIRST	First-order Taylor series	[5, 17]
SECOND	Second-order Taylor series	[28]
CURVE	Second order polynomial curve fitting	[1]
HEURISTIC	Heuristic emphasis on speed or acceleration	[13]
DESP	Double exponential smoothing	[14]
TTP	Derivative estimator with speed threshold	

Table 2: Predictors used in this study. Grey lines represent the predictors used in [20].

We could confirm that hypothesis: as the amount of compensated latency increased, KALMAN was the only predictor in our tests that predicted less and less, i.e. closer and closer to the last detected finger location. We discard KALMAN in the following analysis.

The following simulations are performed as if the predictors were compensating a portion of a fixed end-to-end latency: 68 ms, the same as in the original data. For instance, when the Compensated Latency parameter is set to 24 ms, the side-effect metrics will be calculated using that prediction 24 ms

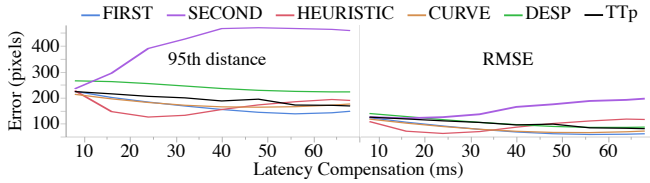


Figure 2: Effects of Compensated Latency and Predictor on typical distance-based error metrics.

in the future against the actual finger position 68 ms in the future. This is different from Appendix II in [20], where metrics were calculated as if every latency was fully compensated.

We optimized the TTP parameters using a sample set of 56 gestures corresponding to 54 seconds of input in total, captured with a high-resolution OptiTrack system. Δ_t was set to 8.33 ms, V_{low} to 102.94 mm/s, and γ_α to 0.73, as defined above. Optimizing for a value of latency takes under 10 min.

Traditional Metrics

We first present the ‘traditional’ metrics used in the literature to evaluate the goodness of predictors: the root-mean-square error (RMSE) and the 95th percentile of the distance between the predicted and the actual finger locations:

Looking for effects of Predictor and Compensated Latency on the error metrics RMSE and 95th distance, we ran a mixed-design analysis of variance for each side-effect, considering participant as random variable using the REML procedure of the SAS JMP package. We found significant effects of Predictor for both RMSE ($F_{5,625} = 207.5, p < 0.0001$) and 95th distance ($F_{5,625} = 557.7, p < 0.0001$). For RMSE, Tukey post-hoc tests found TTP (mean 100.5 px) significantly worse than CURVE (81.7 px) and FIRST (79.1 px), and significantly better than SECOND (158.7 px), with non-significant differences with DESP (104 px) and HEURISTICS (94.2 px). For 95th distance, TTP (193.5 px) was significantly worse than HEURISTICS (170.1 px) and FIRST (167.6 px), and significantly better than DESP (240.6 px) and SECOND (408.4 px), with non-significant differences with CURVE (178.6 px).

We also found significant effects of Compensated Latency for RMSE and of Predictor \times Compensated Latency for RMSE and 95th distance, but will not detail them further than Fig. 2.

The results above would indicate that TTP fares reasonably well overall, but not as good as some, especially FIRST. However Nancel et al. found in [20] that these distance-based metrics can have a strong negative correlation with other side-effects, notably Jitter and Jumps.

We then compared these 6 predictors using the side-effect metrics from [20] described in Table 1. The procedure was twofold, first considering each metric separately, then integrating them all into a generalized score. In both cases, the scores were calculated over the entire dataset, and separately for each participant of the original study.

Scores per Side-Effect

We first compared the predictors on each metric independently, so we could observe specific trade-offs between the

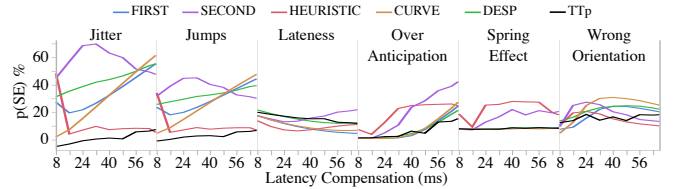


Figure 3: Effects of Compensated Latency and Predictor on the probability to notice each side-effect.

amount of compensated latency and the probability of individual negative side-effect.

Looking for effects of Predictor and Compensated Latency on the probability $p(SE)$ to notice a side-effect, we ran a mixed-design analysis of variance for each side-effect, considering participant as random variable. Unsurprisingly (Fig. 3), we found significant effects of Predictor, Compensated Latency, and Predictor \times Compensated Latency, all $p < 0.001$. We will not detail the later two further than Fig. 3.

What interests us here is how TTP fared against other predictors overall. Post-hoc Tukey tests showed that TTP caused significantly less Jitter (mean 1.6% vs. 11.9 to 56.9%) and Jumps (3.2% vs. 10.8 to 37%) than any other predictor that we tested. It was significantly better on Wrong Orientation (16.1%) than all other predictors (18.7 to 23.8%) except HEURISTIC (14.5%) from which it wasn’t significantly different. It was significantly better on Spring Effect (8.3%) than HEURISTIC and SECOND (resp. 22.3 and 16.3%), and not significantly different from the others (8 to 8.4%). It was significantly better at Over-anticipation (6.8 %) than SECOND, HEURISTIC, and CURVE (resp. 20.8, 19.4, 9.2%), and not significantly different from the others: DESP (8%) and FIRST (8.3%). Finally, for Lateness, TTP (15.5%) was significantly better than SECOND (17.3%), significantly worse than FIRST, HEURISTIC, and CURVE (9.3 to 10.2%), and not significantly different from DESP.

TTP emerges as the most stable predictor (lowest Jitter and Jumps) by a significant margin, i.e. 7 to 36 times lower than other predictors, and belongs to the ‘best’ groups for all side-effects except Lateness. Interestingly, the other ‘best’ predictors often swap rankings depending the side-effect under consideration. For instance, HEURISTIC was comparatively as good for Wrong Orientation but among the worst in Over-anticipation; DESP was among the best in Over-anticipation and among the worst in Jitter. In short, existing predictors trade some side-effects for others, while TTP demonstrates probabilities of side-effects equivalent or lower than the best predictors for most *individual* side-effects.

Overall score

Regarding Lateness, this metric is calculated as the mean of distances between the predicted location of the finger and the actual location of the finger (without latency) when the predicted location is behind the direction of the movement. Predicted points that are ahead are not considered in this calculation: predictors that consistently over-anticipate, e.g. HEURISTIC and CURVE, will fare well at Lateness.

More importantly, Lateness is essentially why prediction occurs in the first place, and therefore the main cause for all the other side-effects. Yet at the same time, it is the side-effect with the lowest Disturbance scores in [20] (Table 1), in which participants reportedly suggested that [perceived] latency was normal, and better than bad prediction errors.

We calculated a general prediction score S_P for each predictor P consisting in the sum of the expected probability $p(SE_P)$ of each side effect SE for this predictor, weighted by the disturbance score $Mo(D)_{SE}$ from Table 1 for that side-effect:

$$S_P = \sum_{SE} p(SE_P) \times Mo(D)_{SE} \quad (6)$$

We used this score to compare the predictors overall in terms of expected overall disturbance:

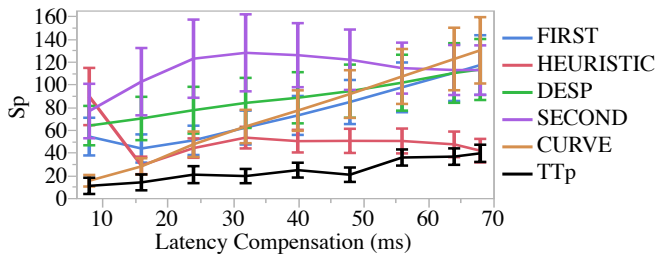


Figure 4: Expected disturbance score per Predictor and Latency Compensation. Error bars are 95% confidence intervals.

Looking for effects of Predictor and Compensated Latency on the overall score S_P , we ran a mixed-design analysis of variance, considering participant as random variable. Unsurprisingly (Fig. 4), we found significant effects of Predictor, Compensated Latency, and Predictor \times Compensated Latency, all $p < 0.001$. We will not detail the later two further than Fig. 4.

What interests us here is how TTP fared against other predictors overall. Post-hoc Tukey tests showed that TTP obtains scores (mean 24.6) significantly lower than any other Predictor overall. HEURISTIC comes second (50.6), significantly lower than any remaining Predictor. CURVE (75.7) is significantly better than DESP (89.1), with FIRST insignificantly different from both. Finally, SECOND obtained scores significantly worse than any other predictor (112.9).

To get a finer picture, we re-ran the above analyses for each amount of Compensated Latency. In each case, there was a significant effect of Predictor ($p < .001$), and Tukey post-hoc tests showed that TTP was either significantly better or non-significantly different from all other predictors in every case.

EXPERIMENT

In order to confirm the results of our benchmark, we ran a controlled experiment on an interactive tablet to gather and compare the opinions of real users on the aforementioned predictors. The experiment involved performing different tasks and different amounts of compensated latency. Participants were asked to rate the acceptability of each condition (Predictor \times Task \times Latency compensation). That yielded significantly more conditions than in [20] (through the Latency compensation factor), so we asked participants to report existing side-effects rather than describe all issues themselves.

Participants

We recruited 9 participants: 2 left-handed, 2 female, aged 22 to 41 (μ 30.8, σ 7.9). All were frequent computer users and used touch input more than one hour per day. Participants were not compensated.

Apparatus

Experiment software was implemented in C++ using Qt 5.9 on an iPad Pro 10.5" (Model A1701) running iOS 11.2. Using Casiez et al.'s method [3], we determined an average 52.8 ms latency (SD 2.8). To get a latency comparable to Nancel et al., who used a Microsoft Surface Pro with an average latency of 72.6 ms [20], we added 20 ms of artificial latency by buffering touch events. In this way we can compare more easily the results of this experiment to the results of the simulations. The iPad Pro's input frequency is 120 Hz, the same as reported in [20].

Conditions

Compensated Latency

We presented participants with five levels of compensated latency: 0, 16, 32, 48, and 64 ms. That is a coarser granularity than in the benchmark above, but allowed us to experiment on different levels of latency compensation while ensuring that the experiment remained in realistic durations.

Tasks

We presented participants with three tasks: **Drawing**, similar to [20], in which participants were instructed to draw a shape that was displayed on the background of the tablet (Fig. 5-a) with their finger at different speeds, along with anything else they wanted; **Dragging**, also similar to [20], in which participants were instructed to drag a square object around with their finger and attempt to drop it within one of four square targets (Fig. 5-b), a task they could repeat as often as they wanted; and **Writing**, in which participants were instructed to write anything they wanted using their finger on the tablet.

Specific minimization objectives such as "click the target as fast as you can" or "follow the shape as precisely as possible" impose constraints on user movements, which in turn might favor—or hide—side-effects caused by slow vs. fast movements, straight vs. curved vs. angled trajectories, etc.; improving performance also does not necessarily mean less noticeable prediction side-effects. We therefore applied the same design as [20], i.e. looser instructions to encourage free exploration of the various conditions and favor larger ranges of "good" and "bad" predictor behaviors. Systematic assessment of performance with TTP is left for future work.

In all tasks the prediction was only used for immediate feedback: last part of the stroke starting from the last detected input for **Writing** and **Drawing**, object location for **Dragging**. Traces, the dragged object's location after release, and stored data if it were a real application, correspond to detected input.

Predictors

The predictors were the same as in the benchmark study: FIRST, SECOND, HEURISTIC, CURVE, DESP, and TTP. The names of the predictors were anonymized ("Technique 1",

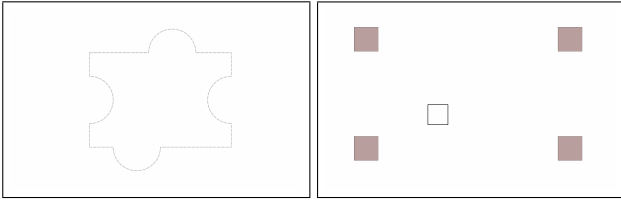


Figure 5: Visual backgrounds of the tasks: (Left) in Drawing, a shape was displayed on the background, including straight and curves lines, and angles. (Right) in Dragging, four target squares were displayed at the corners of the display, slightly larger than the dragged object.

“Technique 2”, etc.). For TTP we ran the optimization described in subsection “Parameters Tuning” above (p.), and calibrated the parameters of the 1€ filter by hand, for each level of latency compensation. As a result of this tuning, filtering was deactivated for 16 ms, the Beta parameter [4] was set to zero in all remaining cases, and the cutoff frequency parameter was set to 45, 20, and 15 Hz respectively for 32, 48, and 64 ms of latency compensation.

Procedure

After being explained the goals and procedure of the experiment, participants were demonstrated each task on the tablet. A trial corresponds to one condition: Predictor, Task, Amount of compensated latency. In each trial, participants were instructed to use the touch interface for as long as they wanted in order to form an opinion regarding (a) whether they noticed issues with the interface, (b) how disturbing those issues were, and whether that would in their opinion prevent its use in a real setting, and (c) which issue was observed among a subset of the side-effects list discussed in [20].

More precisely, after having spent some time in each condition, participants were instructed to:

1. Rate the acceptability of the predictor in that condition on a scale with values “No noticeable issue” (1), “Noticeable issues, but fine” (2), “Some issues, still usable” (3), “Issues, barely usable” (4), and “Unbearable / unacceptable” (5)⁶; that scale mirrors the questionnaire used in [20],
2. Tell whether they would *not* consider using this predictor in daily personal or professional use, and
3. If they would not, list the issues that justify that rejection from a list of side-effects composed of the six described in Table 1, and of two more reported by Nancel et al. as frequently used by their participants [20]:

The acceptability rating set (1. above) is in the form “one neutral, four negatives”, as per the studied problem: our goal is to distinguish levels and types of “imperfection” in the predictions. A perfect prediction feels normal, and can only be observed by comparison to imperfect ones, e.g. through lateness or unwanted interface behaviors.

Random: Could not understand the logic behind some aspects or all of the prediction trajectory.

⁶Participants were presented the rating labels, not the corresponding numbers. For readability we only report numbers in what follows.

Multiple feedback: Seemed like more than one visible feedback at the same time.

Participants could also describe issues that were not in the list, but no other side-effect was reported.

Design

The presentation of the predictors and tasks was counterbalanced using two Latin Square designs, predictors first: all tasks were completed for a given predictor before switching to the next predictor. The ordering of the latency compensation was constant and increasing, from 0 ms to 64 ms.

In the end we obtained ratings and raw input and predicted data for 9 (participants) \times 6 (predictors) \times 3 (tasks) \times 5 (latency) = 810 conditions. The study lasted 1 hour on average for each participant.

Results

We recorded a total of 10,270 strokes but removed the first 5th duration percentile (< 12 ms) and last 5th percentile (> 4629 ms) as Nancel et al. did [20], leaving a total of 9,242 strokes. In each Predictor \times Task condition, participants spent on average 1 min (SD 0.6) interacting with the touch surface (sum of stroke durations). Participants spent on average 2.9 min (1.1) interacting with each Predictor. A multi-way ANOVA reveals that Task had a significant effect on interaction duration ($F_{2,136} = 5, p = .0079$), with **Writing** conditions (mean 0.8 min) taking significantly longer than **Drawing** and **Dragging** (1 min).

Acceptability Ratings

Ratings in absolute value are represented in Fig. 6, aggregated for all participants and all tasks (the lower the better).

As it could be expected, we observe strong discrepancies between the ratings of each participant. For instance, two participants (P3, P7) never used ratings of 4 or above, one (P7) never used the 5th. Conversely, four participants (P5, P7-9) rated all amounts of compensated latency 3 or worse in at least one combination of Predictor \times Task, including with the typical amounts of compensated latencies 0 and 16 ms.

Despite that, visual inspection of the means and confidence intervals (CI) reveal a clear trend in favor of TTP overall, and for amounts of compensated latencies of 32 ms and above. We ran a multi-way ANOVA by treating acceptability ratings as continuous values between 1 and 5 (the lower the better), and modeling participant as a random variable using SAS JMP’s REML procedure. It confirmed that acceptability ratings were significantly affected by Predictor ($F_{5,712} = 53.3, p < 0.0001$), Task ($F_{2,712} = 146.3, p < 0.0001$), and Latency ($F_{4,712} = 243.3, p < 0.0001$), as well as several interaction effects: Predictor \times Latency ($F_{20,712} = 5.8, p < 0.0001$) and Predictor \times Task ($F_{10,712} = 5, p < 0.0001$). TTP (mean 1.61) was found significantly more acceptable than all other predictors (means ≥ 2.41). Unsurprisingly, acceptability ratings increased with the amount of compensated latency, every level being significantly different than the others. Conditions with TTP compensating up to 48 ms of compensation (means 1.33 to 1.7) were found significantly more acceptable than all other predictors at 32 ms (2.48 to 3.15) and above. TTP with up to

64 ms of compensation (2.22) was found significantly more acceptable than all other predictors at 48 ms (3.04 to 3.89) and above.

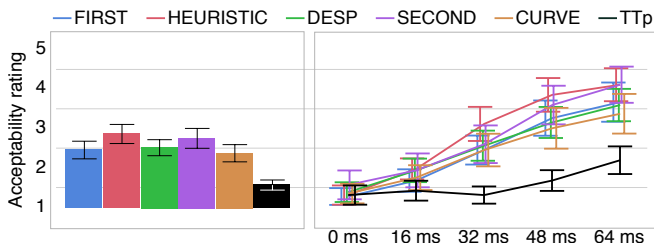


Figure 6: Left: Average ratings for each predictor. Right: Average ratings for each predictor and amount of compensated latency. Error bars are 95% confidence intervals.

Due to the variability in the range of each participant’s responses, we also inspected the *ordering* of these ratings. For each (Participant \times Task \times Latency) combination, we ranked each predictor from best (1) to worst (5). We treated ties ‘optimistically’: equal ratings were considered *ex-æquo* and to the lowest ranking; for instance, if in a given condition the predictors A, B, C, D, E, F had ratings of 1, 1, 2, 3, 4, 4, their corresponding rankings would be 1, 1, 3, 4, 5, 5.

With this method, TTP was ranked first (including ties) 92.6% of the time, second 6.7% of the time, third 0.7% of the time, and never further. By comparison, the other predictors were ranked first 29.6 to 45.2% of the time, second 33.3 to 45.2% of the time, third 12.6 to 28.9% of the time, and fourth 1.5 to 9.6% of the time.

If we break down these rankings per level of compensated latency, we find that TTP was only ever ranked third with 0 ms of compensation. For 16, 32, and 64 ms it was ranked first (incl. ties) respectively 85.2, 92.6, and 96.3% of the time, second the rest of the time. For 48 ms it was always ranked first. Except at 0 ms (where all predictors are equivalent), no other predictor come near this level of plebiscite.

To summarize, TTP obtained consistently better ratings than all other predictors, both in absolute value and in ranking. Participants’ average ratings ranged between 1 (“No noticeable issue”) and 2 (“Noticeable issues, but fine”) in all conditions, including up to 48 and 64 (Fig. 6).

Rejection for Real Use

In each Predictor \times Task \times Latency condition, participants were asked whether they would *not* consider using this predictor at this compensation setting in a similar task, for daily personal use and daily professional use (2 separate questions).

It is not trivial to perform traditional statistical analyses on such a question as a single measure. We cannot simplify it as ‘the lowest level they started rejecting the predictor for that task’ because it happened that participants ticked the box for a given level of latency compensation and not for higher levels. The corresponding data is essentially a binary variable for every combination of Participant \times Predictor \times Task \times Latency, which can only be studied as a whole by considering histograms of responses. In what follows we limit our analysis to an inspection of number of responses.

Similarly to acceptability ratings, we observe a discrepancy between the participants’ tolerance to prediction side-effects. For instance, for personal use, three participants (P2, P5, P8) rejected predictors at least once for each amount of compensated latency, i.e. including when there was no latency compensation at all (0 ms), while five (P1, P3-4, P6-7) only rejected conditions with 32 ms of compensation or higher; two (P3-4) only rejected conditions with 48 ms of compensation or higher. All participants but one (P8) were equally or more tolerant to perceived side-effects when considering personal use than when considering professional use. Counts of rejections are represented in Fig. 7.

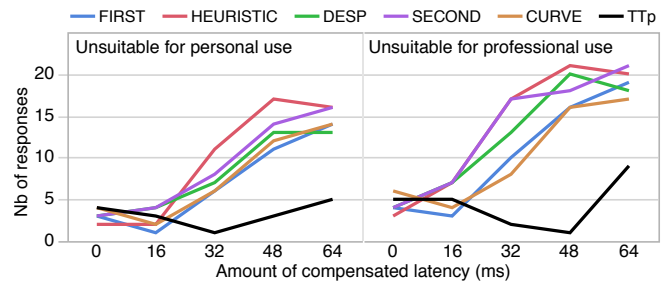


Figure 7: Number of times the participants responded that a particular condition (Predictor \times Task \times Latency) would not be suitable for real use, either personal or professional, by amount of predicted latency.

Upon simple visual inspection, we observe that participants’ rejection of the TTP predictor tends to drop as the level of compensated latency increases, up until 32 and 48 ms for respectively personal and professional use. Rejection of all other predictors steadily increases starting from 0 or 16 ms.

Observed Side-effects

When a participant rejected a given condition, they were instructed to indicate the causes for that rejection. These measures have the same format as above: some participants for example reported “lateness” for low levels of compensation only and other issues starting from e.g. 32 ms. We therefore limit this analysis to an inspection of number of responses. Counts of mentions of each side-effect are shown in Fig. 8.

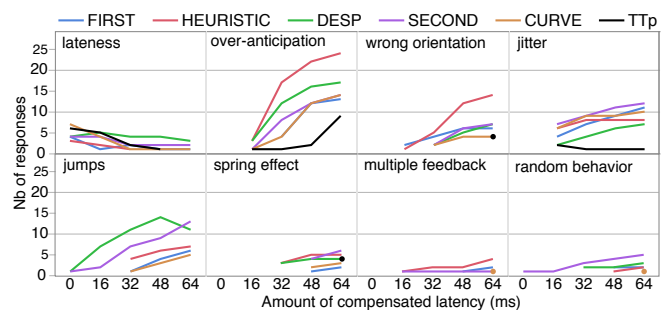


Figure 8: Number of times the participants responded that a particular condition side-effect caused her rejection of a predictor for each level of compensated latency. Single points represent predictors for which a given side-effect was only reported for a unique level of compensation.

We can make several observations: (1) “Jumps” and “Random behavior” are reported at least once for all predictors except TTP; “Multiple feedback” is reported at least once for all predictors except TTP and DESP. (2) “Spring effect” and

“Wrong orientation” are reported for all predictors at least at 48 ms of compensation except for TTP for which it is only reported at 64 ms. (3) “Lateness” has been reported for all predictors, and at all levels of compensation except for HEURISTIC at 48 ms and above, and for TTP at 64 ms; while among the highest for 0 and 16 ms, reports of “Lateness” with TTP quickly drop starting from 32 ms. (4) “Jitter” and “Over-anticipation” were reported at all levels above 0 ms for every predictor, but remain consistently lowest for TTP.

Breaking Down by Task

Inspecting the above results task by task reveals trends similar to [20]. “Lateness” was mostly reported with **Dragging** (77.9% of reports), possibly because the finger was hiding most of the delay (in **Drawing** and **Writing** the prediction was connected to the last detected point by the stroke), and because participants are used to latency in direct touch. “Jitter” and “Jumps” were mostly reported with **Dragging** (resp. 77.2 and 75.2%), again possibly because the finger was hiding most of the trembling—in contrast, the dragged object was larger than the finger. “Over-anticipation” was reported at lower levels of compensation with **Writing** than with the two other tasks: all predictors but FIRST had reports at 16 ms in this task, while in **Dragging** and **Drawing** the reports start at 32, 48, or 64 ms. This is possibly because writing gestures are curvier and, being heavily practiced, faster than drawing and dragging gestures, eliciting brisker responses from the predictors. Finally, “Over-anticipation” was only reported at 64 ms of compensation with TTP for DRAGGING and DRAWING, while for all other predictors it was reported starting at 32 or 48 ms with these tasks.

Comparison with Benchmark Study

The findings from the benchmark and user studies were very similar: TTP was found consistently less disturbing both in theory (benchmark, see e.g. Fig. 4) and in practice (controlled study, Fig. 6-7). Issues of jitter, jumps, and spring effect were very seldom reported (Fig. 8), as predicted (Fig. 3). Reports of over-anticipation stayed low until 48 ms before rising suddenly, in both cases. Finally, some side-effects went even better in practice than predicted: reports of lateness experienced a steady drop starting from 32 ms, and disappeared for 64 ms; and wrong orientation was only observed at 64 ms.

Overall, the results of both studies speak in favor of using TTP at higher levels of latency compensation than the other predictors we tested. Participants ‘rejected’ the use of TTP for professional use less often at 32 and 48 ms of compensated latency than at any other amount, including 0 ms (Fig. 7). All side-effects but lateness, over-anticipation, and jitter were never reported for TTP at these levels of compensation, and the latter three were minimal compared to other predictors. This, we conclude, strongly supports our hypothesis that TTP can be used to forecast direct touch input further in the future than existing approaches.

DISCUSSION AND FUTURE WORK

We presented a new algorithm for next-point input prediction based on three components: (i) a state-of-the-art differentiator to quickly and accurately estimate the instantaneous time

derivatives of the input movement in real time, (ii) a speed-based smoothing mechanism to solve the lateness/jitter trade-off, and (iii) a two-step filtering of the resulting prediction to further decrease jitter without sacrificing angular responsiveness. The effectiveness of the resulting predictor, as demonstrated in a benchmark and a user study, can result from any or all of these components. In effect, the speed-based smoothing and two-steps filtering could theoretically benefit any prediction algorithm. The study of the individual effects of each component is left for future work.

We will also investigate the efficiency of TTP when using other common devices such as direct styli and indirect mice, and whether the calibration processes need to be adjusted in those setups.

Finally, predictors using more complex approaches such as Kalman filters and neuron networks could not be tested in this work for lack of accessible calibration procedures, but those approaches are very promising and we would like to compare them to our predictor in future work.

CONCLUSION

We presented a new prediction technique for direct touch surfaces that is based on a state-of-the-art finite-time derivative estimator, a smoothing mechanism based on input speed, and a two-step post-filtering of the prediction. Using the dataset of touch input from Nancel et al. as benchmark we compared our technique to the ones of the state-of-the-art, using metrics that model user-defined negative side-effects caused by input prediction errors. The results show that our prediction technique presents probabilities of side-effects equivalent or lower than the best predictors for most individual side-effects. This was confirmed in a user study in which participants were asked to rate the disturbance of existing predictors at different levels of latency compensation: our technique shows the best subjectives scores in terms of usability and acceptability. It remains usable up to 32 or 48 ms of latency compensation, i.e. two or three times longer than current techniques.

ACKNOWLEDGMENTS

This work was supported by ANR (**TurboTouch**, ANR-14-CE24-0009).

REFERENCES

1. 2014. Curve fitting based touch trajectory smoothing method and system. <https://www.google.ca/patents/CN103902086A?cl=en> CN Patent App. CN 201,210,585,264.
2. S. Aranovskiy, R. Ushirobira, D. Efimov, and G. Casiez. 2017. Frequency domain forecasting approach for latency reduction in direct human-computer interaction. In *2017 IEEE 56th Annual Conference on Decision and Control (CDC)*. 2623–2628. DOI: <http://dx.doi.org/10.1109/CDC.2017.8264040>
3. Géry Casiez, Thomas Pietrzak, Damien Marchal, Sébastien Poulmane, Matthieu Falce, and Nicolas Roussel. 2017. Characterizing Latency in Touch and Button-Equipped Interactive Systems. In *Proceedings of*

- the 30th Annual ACM Symposium on User Interface Software and Technology (UIST '17)*. ACM, New York, NY, USA, 29–39. DOI : <http://dx.doi.org/10.1145/3126594.3126606>
4. Géry Casiez, Nicolas Roussel, and Daniel Vogel. 2012. 1€ Filter: A Simple Speed-based Low-pass Filter for Noisy Input in Interactive Systems. In *Proc. SIGCHI Conference on Human Factors in Computing Systems (CHI '12)*. ACM, 2527–2530. DOI : <http://dx.doi.org/10.1145/2207676.2208639>
 5. Elie Cattan, Amélie Rochet-Capellan, Pascal Perrier, and François Bérard. 2015. Reducing Latency with a Continuous Prediction: Effects on Users' Performance in Direct-Touch Target Acquisitions. In *Proc. 2015 International Conference on Interactive Tabletops and Surfaces (ITS '15)*. ACM, 205–214. DOI : <http://dx.doi.org/10.1145/2817721.2817736>
 6. Jonathan Deber, Ricardo Jota, Clifton Forlines, and Daniel Wigdor. 2015. How Much Faster is Fast Enough? User Perception of Latency & Latency Improvements in Direct and Indirect Touch. In *Proceedings of the 33rd Annual ACM Conference on Human Factors in Computing Systems (CHI '15)*. ACM, New York, NY, USA, 1827–1836. DOI : <http://dx.doi.org/10.1145/2702123.2702300>
 7. T. E. Duncan, P. Mandl, and B. Pasik-Duncan. 1996. Numerical differentiation and parameter estimation in higher-order linear stochastic systems. *IEEE Trans. Automat. Control* 41, 4 (Apr 1996), 522–532. DOI : <http://dx.doi.org/10.1109/9.489273>
 8. D. V. Efimov and L. Fridman. 2011. A Hybrid Robust Non-Homogeneous Finite-Time Differentiator. *IEEE Trans. Automat. Control* 56, 5 (May 2011), 1213–1219. DOI : <http://dx.doi.org/10.1109/TAC.2011.2108590>
 9. Michel Fliess, Cédric Join, and Hebertt Sira-Ramirez. 2008. Non-linear estimation is easy. *Int. J. Modelling, Identification and Control* 4, 1 (2008), 12–27. DOI : <http://dx.doi.org/10.1504/IJMIC.2008.020996>
 10. Niels Henze, Markus Funk, and Alireza Sahami Shirazi. 2016. Software-reduced Touchscreen Latency. In *Proceedings of the 18th International Conference on Human-Computer Interaction with Mobile Devices and Services (MobileHCI '16)*. ACM, New York, NY, USA, 434–441. DOI : <http://dx.doi.org/10.1145/2935334.2935381>
 11. Niels Henze, Sven Mayer, Huy Viet Le, and Valentin Schwind. 2017. Improving Software-reduced Touchscreen Latency. In *Proceedings of the 19th International Conference on Human-Computer Interaction with Mobile Devices and Services (MobileHCI '17)*. ACM, New York, NY, USA, Article 107, 8 pages. DOI : <http://dx.doi.org/10.1145/3098279.3122150>
 12. Ricardo Jota, Albert Ng, Paul Dietz, and Daniel Wigdor. 2013. How Fast is Fast Enough? A Study of the Effects of Latency in Direct-touch Pointing Tasks. In *Proceedings of the SIGCHI Conference on Human Factors in Computing Systems (CHI '13)*. ACM, New York, NY, USA, 2291–2300. DOI : <http://dx.doi.org/10.1145/2470654.2481317>
 13. B. Kim and Y. Lim. 2014. Mobile terminal and touch coordinate predicting method thereof. <https://www.google.com/patents/WO2014129753A1?cl=en> WO Patent App. PCT/KR2014/000,661.
 14. Joseph J. LaViola. 2003. Double Exponential Smoothing: An Alternative to Kalman Filter-based Predictive Tracking. In *Proc. Workshop on Virtual Environments 2003 (EGVE '03)*. ACM, 199–206. DOI : <http://dx.doi.org/10.1145/769953.769976>
 15. Arie Levant. 1998. Robust exact differentiation via sliding mode technique. *Automatica* 34, 3 (1998), 379 – 384. DOI : [http://dx.doi.org/10.1016/S0005-1098\(97\)00209-4](http://dx.doi.org/10.1016/S0005-1098(97)00209-4)
 16. Jiandong Liang, Chris Shaw, and Mark Green. 1991. On Temporal-spatial Realism in the Virtual Reality Environment. In *Proc. 4th Annual ACM Symposium on User Interface Software and Technology (UIST '91)*. ACM, 19–25. DOI : <http://dx.doi.org/10.1145/120782.120784>
 17. J.S. LINCOLN. 2013. Position lag reduction for computer drawing. <https://www.google.com/patents/US20130271487> US Patent App. 13/444,029.
 18. F. Moussavi. 2014. Methods and apparatus for incremental prediction of input device motion. <https://www.google.ca/patents/US8766915> US Patent 8,766,915.
 19. Tomas Ménard, Emmanuel Moulay, and Wilfrid Perruquetti. 2017. Fixed-time observer with simple gains for uncertain systems. *Automatica* 81, Supplement C (2017), 438 – 446. DOI : <http://dx.doi.org/https://doi.org/10.1016/j.automatica.2017.04.009>
 20. Mathieu Nancel, Daniel Vogel, Bruno De Araujo, Ricardo Jota, and Géry Casiez. 2016. Next-Point Prediction Metrics for Perceived Spatial Errors. In *Proceedings of the 29th Annual Symposium on User Interface Software and Technology (UIST '16)*. ACM, New York, NY, USA, 271–285. DOI : <http://dx.doi.org/10.1145/2984511.2984590>
 21. Albert Ng, Michelle Annett, Paul Dietz, Anoop Gupta, and Walter F. Bischof. 2014. In the Blink of an Eye: Investigating Latency Perception During Stylus Interaction. In *Proceedings of the 32Nd Annual ACM Conference on Human Factors in Computing Systems (CHI '14)*. ACM, New York, NY, USA, 1103–1112. DOI : <http://dx.doi.org/10.1145/2556288.2557037>

22. Albert Ng, Julian Lepinski, Daniel Wigdor, Steven Sanders, and Paul Dietz. 2012. Designing for Low-latency Direct-touch Input. In *Proceedings of the 25th Annual ACM Symposium on User Interface Software and Technology (UIST '12)*. ACM, New York, NY, USA, 453–464. DOI : <http://dx.doi.org/10.1145/2380116.2380174>
23. Wilfrid Perruquetti, Thierry Floquet, and Emmanuel Moulay. 2008. Finite-time observers: application to secure communication. *Automatic Control, IEEE Transactions on* 53, 1 (2008), 356–360. DOI : <http://dx.doi.org/10.1109/TAC.2007.914264>
24. R. Ushirobira, D. Efimov, G. Casiez, N. Roussel, and W. Perruquetti. 2016. A forecasting algorithm for latency compensation in indirect human-computer interactions. In *2016 European Control Conference (ECC)*. 1081–1086. DOI : <http://dx.doi.org/10.1109/ECC.2016.7810433>
25. W.Q. Wang. 2013. Touch tracking device and method for a touch screen. <https://www.google.com/patents/US20130021272> US Patent App. 13/367,371.
26. W. Wang, X. Liu, and G. ZHOU. 2013. Multi-touch tracking method. <https://www.google.com/patents/WO2013170521A1?cl=en> WO Patent App. PCT/CN2012/077,817.
27. Jiann-Rong Wu and Ming Ouhyoung. 2000. On latency compensation and its effects on head-motion trajectories in virtual environments. *The Visual Computer* 16, 2 (2000), 79–90. DOI : <http://dx.doi.org/10.1007/s003710050198>
28. W. Zhao, D.A. Stevens, A. Uzelac, H. Benko, and J.L. Miller. 2012. Prediction-based touch contact tracking. <https://www.google.com/patents/US20120206380> US Patent App. 13/152,991.
29. S.Q. Zhou. 2014. Electronic device and method for providing tactile stimulation. <https://www.google.com/patents/US20140168104> US Patent App. 13/729,048.

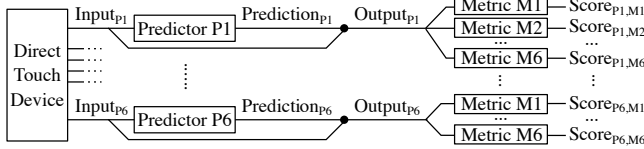
APPENDIX: DATASET VALIDITY

The set of strokes that were used as input in this paper’s benchmark study comes from previous work [20], but to our knowledge such an offline validation has not been tried yet.

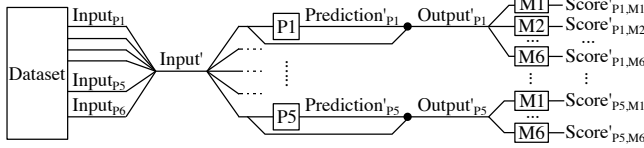
We must first verify a core requirement. Each stroke in this dataset was gathered when a predictor was active (Fig. 9-a). In order to be reusable as realistic input for new predictors, the strokes must be reasonably independent from that predictor, otherwise the simulated behavior of a new predictor using this data as input cannot be generalized.

To this extent, we calculated the predicted input corresponding to each predictor from [20] (gray rows in Table 2), but using strokes from the *entire* dataset. We then calculated the side-effect-modeling metrics in Table 1 using these input+simulated coordinates, for different amounts of compensated latency: 8, 16, 24, 32, 40, 48, 56, 64, and 68 ms. These processes are illustrated in Fig. 9-b,c. In the following we call CAPTURE the predictor that was active at the time of capture of the strokes in the dataset (P_x in Input $_{P_x}$ in Fig. 9), and SIMULATED the predictor we applied to these input strokes in the current process (P_x in Prediction $_{P_x}$ in Fig. 9).

a) Process in [20]:



b) Process in validating the **Independence** of this strokes dataset:



c) Process in validating the **Consistency** of this strokes dataset:

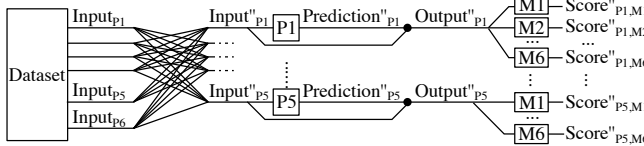


Figure 9: (a) Scores calculated in [20]. (b) Independence test: all input strokes are used to simulate all predictors (except the control condition with no prediction). (c) Consistency test: all input strokes but the ones used in [20] by a given predictor are used to simulate that predictor (except for the control condition). Latencies are not displayed for clarity.

The validity of the dataset to simulate the effects and effectiveness of new input predictors relies on two hypotheses:

Independence: For each metric and each compensated latency, the CAPTURE predictor should not affect the resulting metrics values (Fig. 9-b).

An analysis of variance (ANOVA) investigating the effects of CAPTURE on the probability that users would notice each side-effect ($p(SE)$), for each corresponding metric (6) and each latency (9), found no significant effect in all of the 54 combinations (Fig. 10-left). Note that running the same analysis, but investigating the effects of SIMULATED instead, does find systematic significant effects ($p < .0001$ in all 54 cases, see Fig. 10-right for an example). This is not surprising: different predictors *applied* to a given input dataset are expected to produce different side-effects.

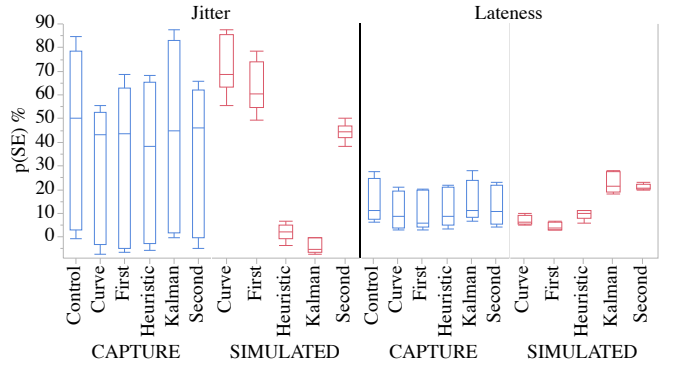


Figure 10: Example effects with the Jitter and Lateness side-effects, for 68 ms of compensated latency.

Consistency: The metric values obtained through simulation, i.e. when CAPTURE \neq SIMULATED (Fig. 9-c), should match the metrics values originally obtained in [20] with CAPTURE.

We define a decision variable ORIGINAL that equals 1 if CAPTURE = SIMULATED and 0 otherwise. An ANOVA investigating the effects of ORIGINAL on the resulting metrics values, for each metric and each latency, found no significant effect in all of the 54 combinations.

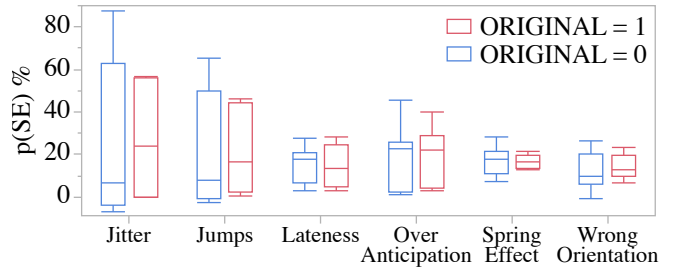


Figure 11: Effect of ORIGINAL for all side-effects for 68 ms of compensated latency.

These results support both the Independence and Consistency requirements, confirming that the data from Nancel et al. can be used to evaluate new predictors.